AMERICAN SOCIETY FOR MICROBIOLOGY | Applied and Environmental Microbiology®

ENVIRONMENTAL MICROBIOLOGY

Heterologous Expression of *Pseudomonas putida* Methyl-Accepting Chemotaxis Proteins Yields *Escherichia coli* Cells Chemotactic to Aromatic Compounds

Clémence Roggo,[a]* Estelle Emilie Clerc,[a,b] Noushin Hadadi,[a] Nicolas Carraro,[a] Roman Stocker,[b] Jan Roelof van der Meer[a]

[a]Department of Fundamental Microbiology, University of Lausanne, Lausanne, Switzerland
[b]Institute for Environmental Engineering, ETH Zürich, Zürich, Switzerland

ABSTRACT *Escherichia coli*, commonly used in chemotaxis studies, is attracted mostly by amino acids, sugars, and peptides. We envisioned modifying the chemotaxis specificity of *E. coli* by expressing heterologous chemoreceptors from *Pseudomonas putida* enabling attraction either to toluene or benzoate. The *mcpT* gene encoding the type 40-helical bundle (40H) methyl-accepting chemoreceptor for toluene from *Pseudomonas putida* MT53 and the *pcaY* gene for the type 40H receptor for benzoate and related molecules from *P. putida* F1 were expressed from the *trg* promoter on a plasmid in motile wild-type *E. coli* MG1655. *E. coli* cells expressing McpT accumulated in chemoattraction assays to sources with 60 to 200 μM toluene, although less strongly than the response to 100 μM serine, but statistically significantly stronger than that to sources without any added attractant. An McpT-mCherry fusion protein was detectably expressed in *E. coli* and yielded weak but distinguishable membranes and polar foci in 1% of cells. *E. coli* cells expressing PcaY showed weak attraction to 0.1 to 1 mM benzoate, but 50 to 70% of cells localized the PcaY-mCherry fusion to their membrane. We conclude that implementing heterologous receptors in the *E. coli* chemotaxis network is possible and, upon improvement of the compatibility of the type 40H chemoreceptors, may bear interest for biosensing.

IMPORTANCE Bacterial chemotaxis might be harnessed for the development of rapid biosensors, in which chemical availability is deduced from cell accumulation to chemoattractants over time. Chemotaxis of *Escherichia coli* has been well studied, but the bacterium is not attracted to chemicals of environmental concern, such as aromatic solvents. We show here that heterologous chemoreceptors for aromatic compounds from *Pseudomonas putida* at least partly functionally complement the *E. coli* chemotaxis network, yielding cells attracted to toluene or benzoate. Complementation was still inferior to native chemoattractants, like serine, but our study demonstrates the potential for obtaining selective sensing for aromatic compounds in *E. coli*.

KEYWORDS biosensing, chemotaxis

Chemotaxis is a rapid (second-scale) behavior of motile organisms to swim toward an attractant or away from a repellent. Chemotactic bacteria can produce a variety of chemoreceptors, some of which have high chemical specificity and selectivity, and others reacting more broadly to related compound classes (1). Chemotaxis could thus be an interesting property for the development of bacterium-based biosensors, which might eventually be deployed to detect and quantify chemical targets in samples (2, 3).

Chemotaxis of *Escherichia coli* is strong and highly reproducible with known and potent chemoattractants, such as serine or aspartate, and has been widely studied (4, 5). Unfortunately, *E. coli* does not naturally display chemotaxis toward molecules of

Received 4 June 2018 **Accepted** 5 July 2018
Accepted manuscript posted online 13 July 2018
Citation Roggo C, Clerc EE, Hadadi N, Carraro N, Stocker R, van der Meer JR. 2018. Heterologous expression of *Pseudomonas putida* methyl-accepting chemotaxis proteins yields *Escherichia coli* cells chemotactic to aromatic compounds. Appl Environ Microbiol 84:e01362-18. https://doi.org/10.1128/AEM.01362-18.
Editor Rebecca E. Parales, University of California, Davis

Address correspondence to Jan Roelof van der Meer, janroelof.vandermeer@unil.ch.
* Present address: Clémence Roggo, University of Applied Sciences and Arts, Western Switzerland, Changins, Nyon, Switzerland.

potential interest for environmental monitoring, such as aromatic or chlorinated solvents. Given its relatively narrow native chemoattractant range, it is interesting to investigate whether the *E. coli* chemotaxis system can be complemented by heterologous chemoreceptors. One important characteristic of methyl-accepting chemotaxis proteins (MCPs) and chemotaxis effector proteins (e.g., CheY) is their structural conservation among bacteria (6–8). *E. coli* possesses five chemotaxis receptors, but other environmental bacteria frequently encode many more chemoreceptors, albeit with often-unknown effectors. For example, *Pseudomonas* species can encode more than 20 MCPs in their genomes (9, 10). A few studies have demonstrated successful expression of heterologous chemoreceptors in *E. coli*. For example, several MCPs from *Shewanella oneidensis* could be expressed in *E. coli*, enabling energy taxis with nitrate (11). Also, Aer-2, a soluble receptor from *Pseudomonas aeruginosa* with an unclear function, and PctApp, a putative MCP for amino acids from *Pseudomonas putida*, were shown to partially trigger chemotaxis response when expressed in *E. coli* (12, 13). However, no MCPs involved in sensing of environmental pollutants have to date been functionally expressed in *E. coli*.

As part of the characterization of bacterial biodegradation pathways, several bacteria were shown to be chemotactic to aromatic compounds, such as to naphthalene, toluene, benzoate, or 2,4-dichlorophenoxyacetic acid (14–17). Some bacteria have been characterized in some detail as to their MCPs and chemical effector(s). For example, an MCP named McpT was identified on the self-transmissible plasmid pGRT1 in *P. putida* DOT-T1E, which enables chemotaxis to toluene and naphthalene (18, 19). This *mcpT* gene may be more widespread among pseudomonads, as it possesses 99.8% sequence similarity to coding sequences on the toluene (TOL) plasmid pWW53 of *P. putida* MT53 (19). Strain MT53 was mentioned as a moderate chemotactic responder to toluene. Further chemoreceptors have been characterized in *P. putida* F1. As an example, the PcaY receptor was shown to be involved in chemotaxis toward vanillate, vanillin, 4-hydroxybenzoate, benzoate, protocatechuate, quinate, and shikimate (20).

The primary goal of this work was to investigate whether chemotaxis specificity of *E. coli* could be expanded toward aromatic compounds. This could be used as proof of concept for the future development of biosensing strains of *E. coli* that are selectively chemotactic toward environmental pollutants for deployment in quantitative biosensor microfluidic platforms (3). Our strategy was to express the *mcpT* gene from *P. putida* MT53(pWW53) or the *pcaY* gene from *P. putida* F1 on a selectable plasmid in motile *E. coli* wild-type MG1655 and in a mutant background in which the gene for the major chemoreceptor Tsr was deleted, and to compare chemotaxis to toluene or benzoate with chemotaxis to serine or to no attractant in strains expressing or not the *mcpT* or *pcaY* gene. Compound-specific chemotaxis was quantified in two manners: first, by microscopy and image analysis from cell accumulation nearby solid agarose sources containing the respective chemoattractant; and second, by a recently developed *in situ* chemotaxis microfluidic assay (ISCA) (21). Subcellular localization of the heterologous MCP receptors was assessed and quantified from expressed equivalent mCherry-fusion proteins in *E. coli* observed by epifluorescence microscopy, in comparison to that of a Tsr-mCherry fusion.

RESULTS

Chemotactic response of *E. coli* to attractants in agarose plug assays. In order to quantify *E. coli* chemotaxis to different molecules, we used two independent assays, microscopy observation of cell accumulation to chemoattractants diffusing from a solid agarose source, and a microfabricated *in situ* chemotaxis assay (ISCA). The agarose plug assays in microscope settings (22) embed the test compound in a solidified cylinder (ø, 4 mm; height, 0.15 mm) of agarose (the source), while introducing a homogenous *E. coli* cell suspension in motility buffer around the source (Fig. S1 in the supplemental material). The bacterial accumulation nearby the source edge was recorded by phase-contrast microscopy after 15 min of incubation at 21°C and quantified using image analysis (Fig. S1). Robust chemotaxis of *E. coli* MG1655 was detected to the known

chemoattractants serine, aspartate, and methylaspartate at 10 and 100 μM source concentrations (Fig. 1A and B). In contrast, cell accumulation of *E. coli* MG1655 to the weaker chemoattractants ribose or galactose at 10 or 100 μM was not statistically significantly different from cells accumulating on the edge of agarose sources without any attractant added (Fig. 1C). These results indicate that the agarose plug assay protocol can be used to measure *E. coli* attraction to chemical targets with a "strength of attraction" in between ribose/galactose and serine/aspartate/methylaspartate.

Chemotaxis of *E. coli* expressing the McpT protein of *P. putida*. Chemotaxis to toluene was tested in motile *E. coli* MG1655 expressing the *mcpT* gene from plasmid pWW53 of *P. putida* MT53 (23) on plasmid pSTV28. In first instance, the *mcpT* gene was expressed from the low constitutive synthetic P_{AA} promoter (24), but this yielded only few viable transformants that always contained mutations in *mcpT*, causing frameshifts leading to a premature stop codon or a deletion. In contrast, expression of the *mcpT* gene on plasmid pSTV28 from the *trg* promoter (also controlling transcription of the native Trg chemoreceptor in *E. coli* [25]) resulted in many viable transformants with correct sequences of *mcpT*. This indicated that we could achieve the expression of McpT in *E. coli* using the *trg* promoter.

Observation of attraction to toluene is complicated by the technical difficulties to produce a solid source containing toluene, which is poorly soluble in water and volatile. First attempts using toluene dissolved in eicosane or dimethyl sulfoxide before mixing with agarose were unsuccessful. We could improve consistency by mixing small volumes of liquid toluene directly with dissolved agarose at 55°C inside completely filled and closed glass vials. Indeed, *E. coli* cells expressing McpT from the *trg* promoter on plasmid pCRO20 incubated in motility buffer accumulated close to a solid agarose source with 60 μM toluene (Fig. 2A and B). The accumulation of cells in response to toluene was less pronounced than that in response to a 100 μM serine source but statistically significantly higher than that with sources without any attractant added (Fig. 2A and B; one-way analysis of variance [ANOVA] and multiple comparison, $P = 0.0119$). Accumulation was robust across 4-fold replicates, and experiments were carried out independently on different days (Fig. 2B). The variation in the magnitude of accumulation was more important with toluene ($\pm$31% of the average) than with serine ($\pm$3%, Fig. 2B inset), which is likely due to the variation in preparing consistent sources with a volatile attractant. At a 10-fold-lower toluene source concentration (6 μM), cell accumulation of *E. coli*(pCRO20) at the source edge was no different from a source without anything added (Fig. 2B, inset). A 10-fold higher source concentration of toluene (600 μM) did not result in cells accumulating near the source surface, even though the cells were visibly still motile and able to swim in proximity to the source (data not shown).

In contrast to *E. coli* cells expressing McpT, cells of both *E. coli* containing the empty plasmid pSTV28 and *E. coli* carrying a plasmid with a frameshift mutation in the *mcpT* coding sequence causing premature ending (pCRO35) did not accumulate toward a 60 μM toluene source to a higher degree than to a source without attractant added (Fig. 2C and D and S2). Both strains, however, responded as expected to a 100 μM serine source and thus were chemotactic (Fig. 2C and D).

Chemotactic response of *E. coli* expressing the PcaY receptor for benzoate. In separate experiments, we expressed in motile *E. coli* MG1655 the gene for the PcaY receptor from *P. putida* F1, which has been reported to induce chemotaxis to molecules, such as vanillate, vanillin, 4-hydroxybenzoate, benzoate, protocatechuate, quinate, and shikimate (20). Cells of *E. coli* MG1655(pCRO33) expressing PcaY from the *trg* promoter accumulated nearby a source plug with 1 mM benzoate. The response was weaker than the response to 100 μM serine but stronger than that to a source without added attractant (Fig. 3A). A lower concentration of benzoate (0.1 mM) decreased cell accumulation to a level no different from that observed without attractant added (Fig. 3A). Cells of *E. coli* MG1655(pSTV28) (without *pcaY*) also accumulated nearby a 1 mM benzoate source, with an intensity similar to that of MG1655(pCRO33) (Fig. 3B). Cell

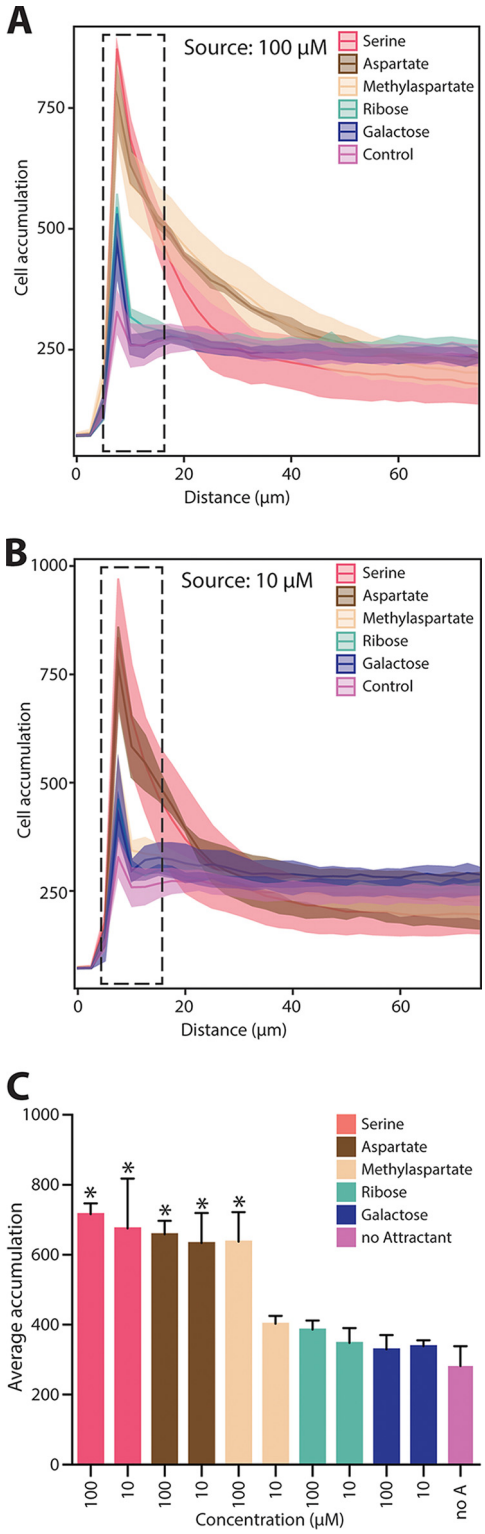

FIG 1 Chemotaxis response of *E. coli* MG1655 toward various common attractants in agarose plug assays. (A) Average cell accumulation of *E. coli* MG1655 as a function of distance from the source edge with 100 μM serine, aspartate, methylaspartate, ribose, galactose, or a no-attractant control. Ribbon traces show the average of triplicates (central line) $\pm$ one standard deviation (bordering lines). (B) Same as in panel A but with source concentration of 10 μM of the different attractants. (C) Average gray values across the three zones closest to the source edge (7.5-μm width) summarized for the different attractants and concentrations. Asterisks indicate significantly different values at a P value of <0.0001 in one-way ANOVA, followed by Tukey *post hoc* multiple-comparison test. Dashed boxes indicate the distance zones used for calculating cell accumulation.

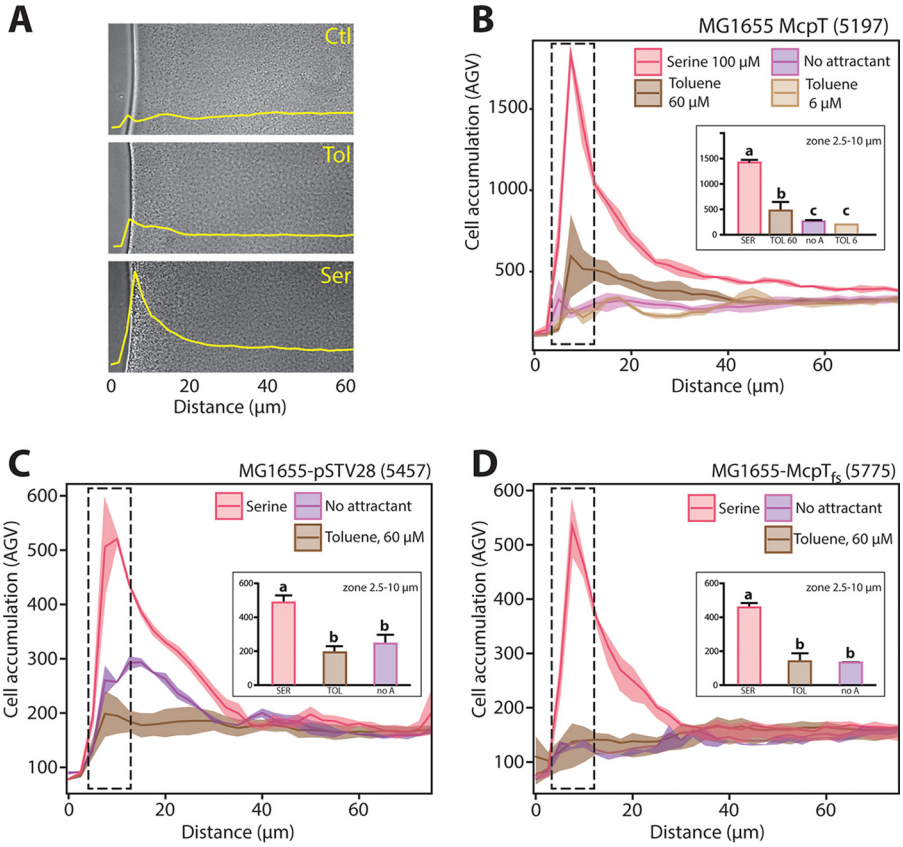

FIG 2 Chemotaxis of *E. coli* expressing *mcpT* of *P. putida* toward toluene. (A) Cropped 100-fold magnification phase-contrast images of one agarose plug replicate experiment with sources containing no attractant (Ctl), 60 μM toluene (Tol), or 100 μM serine (Ser). Yellow curves represent the measured cell accumulation. Note the agarose sources localized on the left of the images, with the source edge typically resulting in a dark-light band. (B) Average cell accumulation (as image average gray values [AGV]) as a function of distance from the source edge averaged from four biological replicates imaged on both sides of the agarose plug with toluene (6 μM [TOL 6] and 60 μM [TOL 60]), serine (SER; 100 μM), or a no-added-attractant control for *E. coli* MG1566(pCRO20) expressing the McpT receptor from *P. putida* MT53 (no A). Ribbon traces show the average of four replicates ± one standard deviation. Inset shows the average gray value across the three zones closest to the source edge (7.5-μm width). Letters indicate significance groups in a one-way ANOVA, followed by *post hoc* Tukey multiple-comparison test. (C) Same as in panel B but with *E. coli* MG1655(pSTV) (empty plasmid). (D) Same as in panel B but with *E. coli* MG1655(pCRO35), which contains a frameshift mutation in *mcpT* causing a premature translation stop. Dashed boxes indicate the distance zones used for calculating cell accumulation.

accumulation of *E. coli* MG1655(pCRO33) to sources of 4-hydroxybenzoate and vanillate (at 0.1 and 1 mM) was not significantly different than that to a source without attractant added.

Chemotactic cell accumulation in microfabricated wells. As a second independent method for chemotaxis quantification, we deployed the recently developed ISCA (21). The ISCA consists of five replicates of ~110-μl wells, fabricated out of the biocompatible polymer polydimethylsiloxane (PDMS) bonded to a glass slide. The wells are filled with a chemoattractant solution and then immersed in a dilute cell suspension (2×10^6 to 4×10^6 cells · ml^{-1}). A single acentrically placed port (ø, 0.8 mm) functions as an inlet channel through which the chemoattractants diffuse out to form gradients and through which motile chemotactically attracted cells can enter the wells. Washed *E. coli* MG1655 wild-type motile cells suspended in motility buffer (strain 4498) accumulated up to 5-fold inside the ISCA cavities within a 35-min incubation period with 100 or 300 μM serine as an chemoattractant, in comparison to motility buffer (MB) alone (Fig. 4A). In contrast, cells did not statistically significantly accumulate to benzoate at 100 or 300 μM concentrations in comparison to MB but were statistically

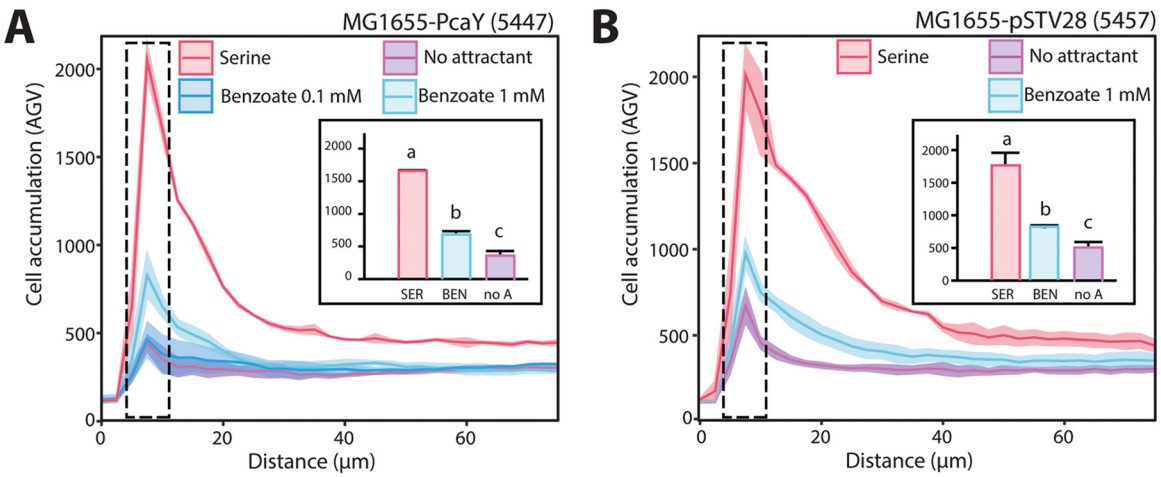

FIG 3 Chemotaxis response of PcaY expressing *E. coli* MG1655. (A) Cell accumulation as a function of distance to an agarose plug with benzoate (1 or 0.1 mM), serine (100 μM), or no attractant of *E. coli* MG1566(pCRO33) expressing the PcaY receptor for benzoate of *P. putida* F1. (B) Same as in panel A for *E. coli* MG1566(pSTV) (empty plasmid). Cell accumulation, ribbon traces, and dashed boxes and inset are the same as described in the legend to Fig. 2. The benzoate source concentration is 1 mM for the data shown in the inset.

significantly repelled at higher benzoate concentrations (300 and 1,000 μM) and by toluene at 60 and 200 μM dosages (Fig. 4A). *E. coli* MG1655 cells expressing the McpT receptor (plasmid pCRO20, strain 5197) consistently accumulated inside ISCA wells filled with serine (100 and 300 μM), as well as with toluene at 60 and 200 μM (~3-fold), but not with benzoate (300 μM), in comparison to MB (Fig. 4B). Cells were not attracted to a higher concentration of toluene (600 μM, Fig. 4B). *E. coli* MG1655 cells expressing PcaY from plasmid pCRO33 (strain 5447) were attracted to serine, as expected, and slightly (1.2-fold) to 300 μM benzoate, although this was not statistically significant from that with MB alone (Fig. 4C), as a result of larger variation across replicates. Strain 5447 cells were repelled by high benzoate concentrations but not by toluene (Fig. 4C). However, in an *E. coli* MG1655 motile background in which the major chemoreceptor Tsr (for serine) was deleted and PcaY was expressed, accumulation to serine was largely absent, and a statistically significant response to benzoate was observed (1.5-fold; Fig. 4D). Expression of McpT from plasmid pCRO20 in the *E. coli* Δ*tsr* mutant background yielded cells no longer accumulating to serine, but attraction to toluene did not further improve (1.7 times accumulation at a 200 μM toluene dosage; Fig. 4E).

Localization of the expressed *P. putida* MCPs in *E. coli*. In order to further demonstrate whether McpT and PcaY are functionally produced in *E. coli*, their coding regions were translationally fused with that for mCherry (without start codon itself). The fusion genes were cloned and again expressed under the *trg* promoter on plasmid pSTV28 (Fig. S2 and S3) in either the *E. coli* MG1655 motile wild type or the Δ*tsr* mutant background. As a positive control, we used *E. coli* MG1655 cells expressing a Tsr-mCherry fusion protein from the *trg* promoter on plasmid pSTV28. These cells showed bright fluorescence, which was enriched in the membrane and in broad zones near the cell poles (Fig. 5B). An *E. coli* control expressing Tsr alone (without mCherry) was not fluorescent (Fig. 5A). Projection of detectable foci (see Materials and Methods for detection of foci) as well as overall pixel intensities across all imaged cells normalized to a standardized *E. coli* cell length (Fig. 6A and B), showed the strong overall polar localization of the Tsr-mCherry fusion protein. This is in agreement with findings from previous studies and what is expected for the localization of the major *E. coli* chemoreceptors (26, 27). *E. coli* cells expressing McpT-mCherry were on average more fluorescent than *E. coli* MG1655, MG1655 expressing McpT alone (without mCherry), or MG1655 expressing a frameshifted *mcpT-mCherry* (Fig. 5C to E, note fluorescence scales). A small proportion of cells (~1%) contained confined (but rather weak) fluorescent foci in the membrane (Fig. 5C, arrows). Superposed projection of all detected

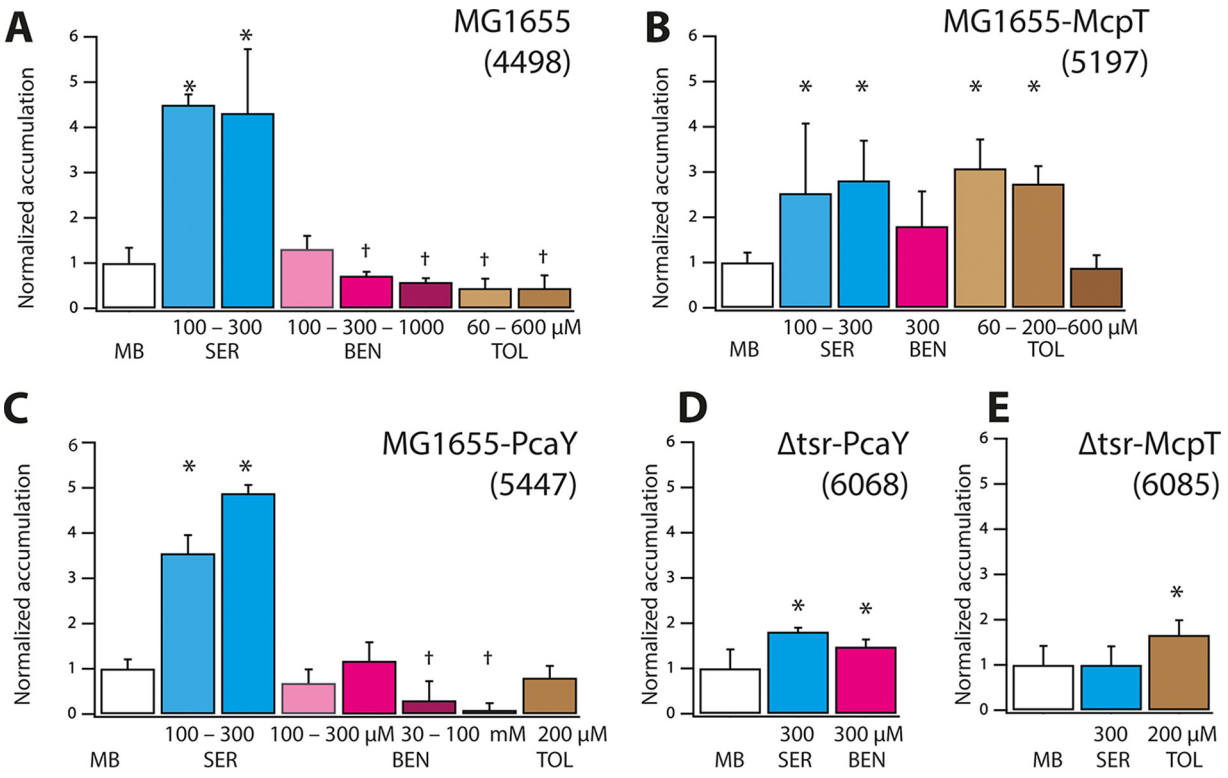

FIG 4 *E. coli* cell accumulation in wells of an *in situ* chemotaxis microfabricated chip. (A to E) *E. coli* MG1655 wild type (strain 4498) (A), *E. coli* MG1655(pCRO20) expressing McpT (strain 5197) (B), *E. coli* MG1655(pCRO33) expressing PcaY (strain 5447) (C), *E. coli* MG1655 Δ*tsr*(pCRO33) expressing PcaY (strain 6068) (D), *E. coli* MG1655 Δ*tsr*(pCRO20) expressing McpT (strain 6085) (E). Bars show average cell accumulation plus standard deviation (SD; error bars) to the indicated chemoattractants measured by absolute flow cytometric counting across 5-fold replicate cavities, normalized to that of cavities filled with motility buffer (MB) alone. Note that panels may be composed of different independent experiments, which are normalized to the respective cell accumulation in MB as a control for every individual chemotaxis assay. SER, serine; BEN, benzoate; TOL, toluene. Concentrations are in micromolar or millimolar, as indicated. Asterisks and daggers denote significantly increased and decreased responses, respectively, compared to motility buffer at P values of <0.05 in pairwise t tests.

fluorescent foci across imaged cells showed that McpT-mCherry expression was localized in the membrane area of the cells and the poles (Fig. 6A). Cells expressing truncated McpT-mCherry still displayed some fluorescence, which might be the result of a start codon downstream of the frameshift position in *mcpT*, but they never produced any visible foci (Fig. 5D). Projection of detected foci produced very few and spurious spots across many cells of both *E. coli* expressing McpT without mCherry fusion and the frameshifted McpT-mCherry (Fig. 6A). Enrichment of McpT-mCherry foci near the cell poles was clearer in an *E. coli* Δ*tsr* mutant background (Fig. 6A). We further quantified mCherry-fusion protein expression by recording the mean intensity of the top 10% brightest pixels per cell, normalized to the mean fluorescent brightness over all individual cells (Fig. 6C). The mean top 10% fluorescence was statistically significantly higher in *E. coli* wild type and Δ*tsr* mutant background expressing McpT-mCherry than in *E. coli* expressing McpT or the frameshifted McpT-mCherry (Fig. 6C).

E. coli expressing *pcaY-mCherry* showed, on average, brighter fluorescence localization in the cellular membrane and more frequently at the cell poles than *E. coli* expressing McpT-mCherry (Fig. 5F and 6A), as well as in a higher proportion of cells (50 to 70%), and with the top 10% fluorescence being clearly higher (Fig. 6C). The fluorescence of the expressed PcaY-mCherry was less bright than in the case of Tsr-mCherry (Fig. 5B and 6C), but its localization was similar (Fig. 6A). The expression of PcaY-mCherry in a Δ*tsr* background increased the top 10% fluorescence level of cells, suggesting higher expression and or more appropriate oligomerization.

These results thus confirmed that the McpT- and PcaY-mCherry receptors are expressed in *E. coli* and are preferentially localized to the cell membrane and poles. In

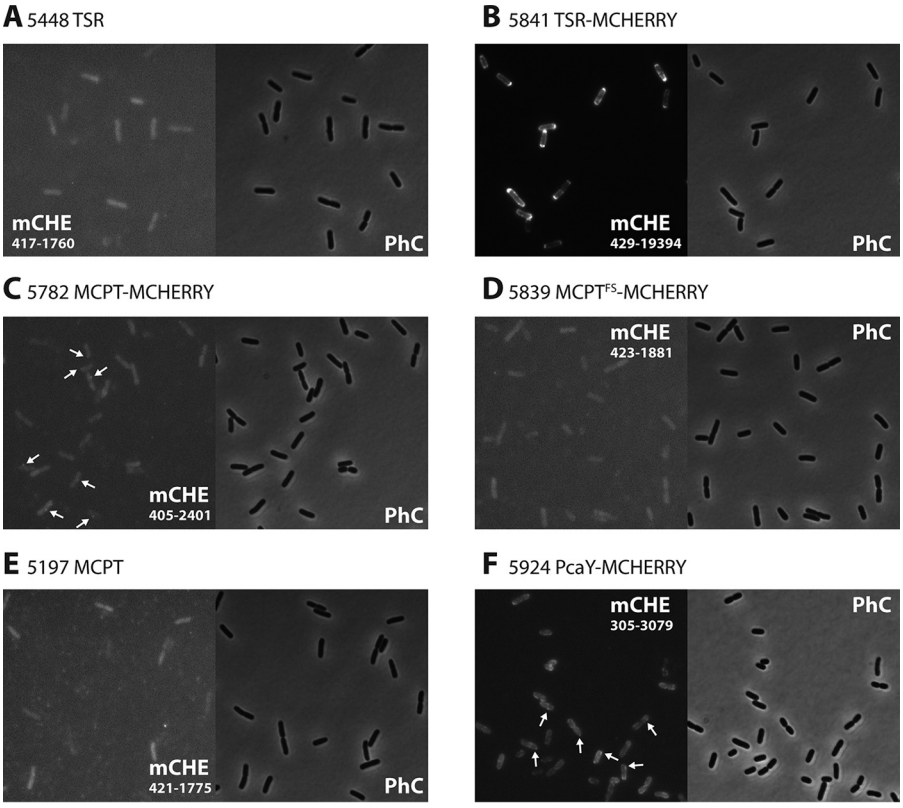

FIG 5 Characterization of MCP receptor expression in *E. coli* by fluorescent protein fusions. (A to F) Phase-contrast (PhC) and mCherry (mCHE) epifluorescence images of *E. coli* MG1655(pCRO34), expressing the Tsr receptor (TSR) (A), MG1655(pCRO38), expressing a Tsr-mCherry fusion protein (TSR-MCHERRY) (B), MG1655(pCRO36), expressing a fusion protein of McpT and mCherry (MCPT-MCHERRY) (C), MG1655(pCRO37), expressing an mCherry fusion protein but with a frameshift mutation in *mcpT* coding sequence (MCPT^{FS}-MCHERRY) (D), MG1655(pCRO20) expressing McpT (MCPT) (E), and MG1655(pCRO33-mCHE), expressing the PcaY-mCherry fusion protein (F). (C and F) Arrows show visible membrane foci of McpT-mCherry and PcaY-mCherry. Images were recorded and autoscaled in ImageJ, saved as 8-bit grayscale for reproduction, opened and cropped to their final size in Adobe Photoshop (version CC2017), and finally saved as .TIF with 300 dpi resolution for display. Numbers in fluorescence images indicate the absolute intensity scaling (minimum to maximum) for reproduction.

contrast to expression of Tsr- and PcaY-mCherry, the proportion of *E. coli* cells with visibly localized McpT-mCherry fluorescence was low (~1%).

DISCUSSION

Heterologous expression of chemoreceptors and functional complementation of chemotaxis in *E. coli* is not straightforward, and relatively few studies have examined them (11, 13). The major aim of this work was to investigate the possibility to functionally express chemoreceptors for detection of the aromatic compounds from *P. putida* in motile *E. coli* cells. We focused on two chemoreceptors, McpT (18, 19) and PcaY (20), which from studies in their native host or by analogy were reported to detect and signal the presence of toluene and benzoate (plus a further range of substituted aromatic compounds), respectively. By using two different chemotaxis assays and by studying the expression and subcellular localization of chemoreceptor-mCherry fusion proteins, we conclude that both chemoreceptors are functionally expressed in *E. coli* and can lead to chemotaxis of motile *E. coli* cells toward toluene or benzoate at source concentrations in the range of 60 to 300 μM. Accumulation was concentration dependent, which is a hallmark of chemotaxis. But the range of source concentrations yielding measurable cell accumulation was relatively narrow, which may be due to toxicity or repellent response at higher chemoattractant concentrations.

Chemotaxis of *E. coli* cells expressing the heterologous chemoreceptors McpT or

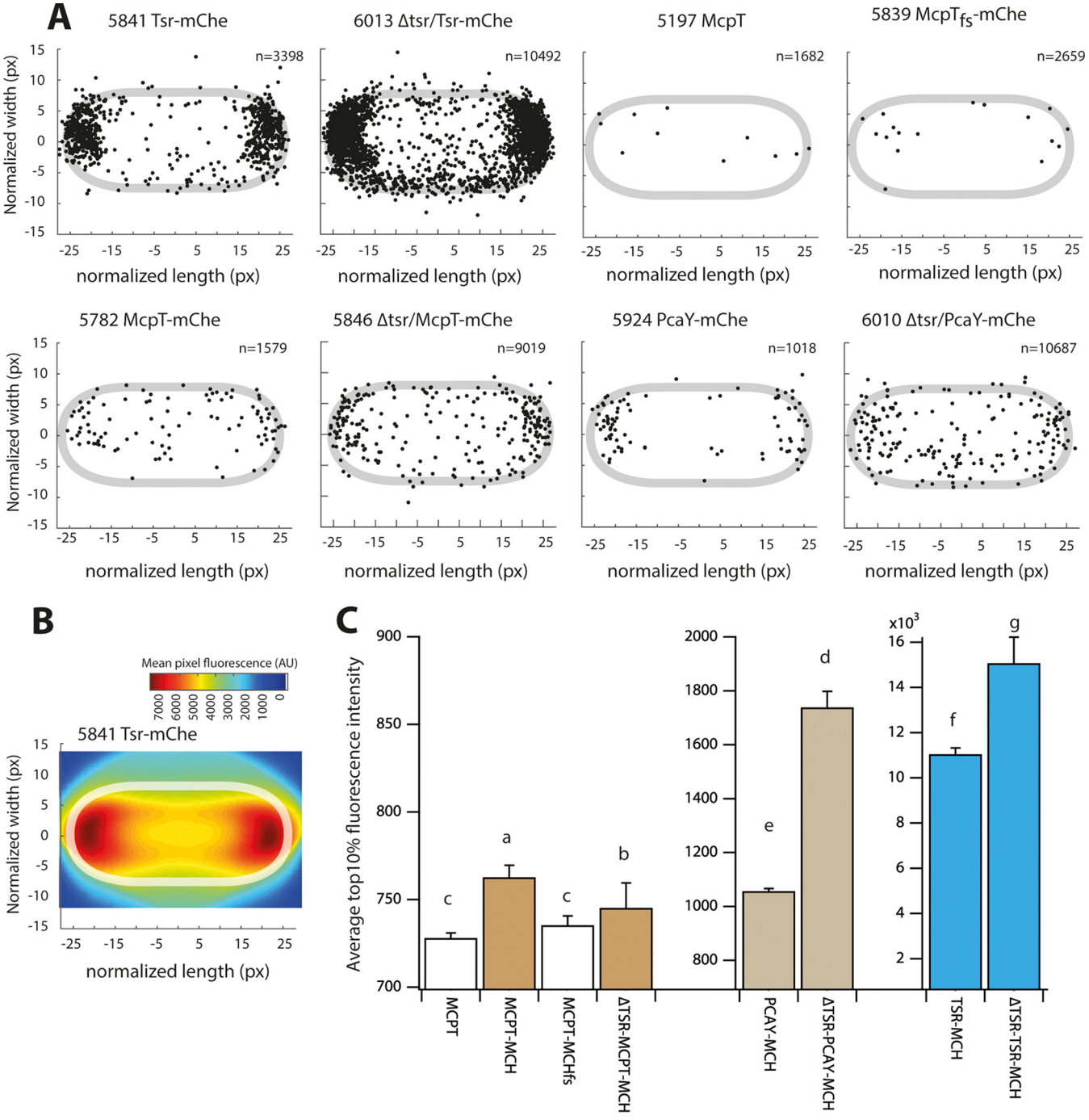

FIG 6 Localization and quantification of chemoreceptor-mCherry fluorescent protein fusions in *E. coli*. (A) Positions of fluorescent foci (black dots) in *n* individual cells extracted by SuperSegger from image series in the different strains (as indicated), superposed, and plotted on a standardized *E. coli* cell by a MatLab custom subroutine. px, pixels. (B) Heatmap of fluorescent pixel intensity extracted from 1,000 *E. coli* cells showing the position of Tsr-mCherry fluorescence normalized to a standardized cell length and width. (C) Average top 10% pixel intensity per cell among *n* cells as from panels A to H, normalized to the mean fluorescence intensity of all cells of that strain. Error bars show SD of 10 images. Note the different intensity scales between strains expressing McpT derivatives, PcaY-mCherry, and Tsr-mCherry. Letters above bars indicate statistically significantly different categories in ANOVA, followed by Tukey *post hoc* testing ($P < 0.005$).

PcaY is relatively weak compared to its major chemoattractant serine. This may be due to the small proportion of cells correctly expressing and localizing the McpT or PcaY chemoreceptors (Fig. 6A to H) and to a general poor compatibility of this class of chemoreceptors with *E. coli* downstream signaling proteins CheA and CheW. According to the chemoreceptor classification of Alexander Zhulin (6), McpT and PcaY belong to

the 40-helical bundle (40H) type, whereas the *E. coli* MCPs (like Tsr and Tar) are part of the 36H type. Although the two chemoreceptor types have strong sequence conservation in the signaling domain (Fig. S4), with conserved amino acids at positions known to be contacted by CheA and CheW (28), notably, the positions of methylation sites are partly different or absent in the 40H type, and the nature of the residue for interdimer trimerization of Tsr (Phe-373) is charged instead of hydrophobic in the 40H type (6). The consequence of this may be different oligomerization arrangements of expressed 40H-type chemoreceptors in *E. coli* and poorer downstream signaling.

Despite this, detectable fluorescent foci and fluorescent membrane zones in *E. coli* cells (Fig. 6) indicated that McpT-mCherry and PcaY-mCherry are mostly localized in the membrane and cell poles. The expression of McpT- and PcaY-mCherry was much weaker than that of Tsr-mCherry expressed from the same *trg* promoter on plasmid pSTV, even in an *E. coli* host devoid of Tsr, although the average top 10% pixel fluorescence further increased in the *E. coli* Δ*tsr* mutant compared to the wild type (carrying pCRO33) with *pcaY-mCherry* (Fig. 6C). When assuming that the localization of McpT and PcaY is analogous to that of their -mCherry counterparts, these results are a further sign that their folding or membrane oligomerization is not optimal for *E. coli*. The relatively small proportion of cells with visible McpT-mCherry foci (~1%, Fig. 5C) might be an indication that only a small subpopulation of *E. coli* actually is responsive to toluene, which would explain the relatively poor overall accumulation of motile cells in suspensions. Our results are thus in agreement with those from previous studies demonstrating successful heterologous expression in *E. coli* of other nonnative type 40H receptors, such as the PctApp serine receptor of *P. putida* (13) or the nitrate energy-taxis MCPs from *S. oneidensis* (11). Expression of the PctApp receptor from a salicylate-inducible system yielded at least partially proper protein-protein interactions to *E. coli* CheA and CheY, although cell accumulation was only observed at 10 mM serine (13). Type 40H chemoreceptors thus seem to connect to the *E. coli* chemotaxis signaling pathways but with lesser efficiency in attractant-biased motility.

One of the issues when studying heterologous chemoreceptor expression in *E. coli* and its correspondingly weaker or different chemotactic behavior is the poor sensitivity and reproducibility of most traditional chemotaxis assays, such as capillary assays, swimming plates, or source accumulation assays. We showed here how cell accumulation to chemoattractants at concentrations of the order of 100 μM can be more accurately quantified from microscopic agarose plug assays with standard errors in the order of 5% of the mean (Fig. 1). Cell accumulation in the wells of the ISCA device across five replicates was slightly more variable (standard error, ~15% of the mean), which is most likely due to the lower concentration of cells used (2×10^6 to 4×10^6 versus 10^9 cells $\cdot$ ml^{-1}), or possibly to small differences in the geometry of the wells or fluid motion while incubating the cell suspension. We noted additional effects on the outcome of the ISCAs related to different growth temperatures of the *E. coli* culture (30°C or 37°C), the cell treatment procedure (washing in motility buffer or not), and assay incubation temperature (preheating culture media). ISCAs confirmed previous studies that benzoate is a repellent for *E. coli* and *Salmonella* spp. (29) but only at concentrations above 300 μM (Fig. 4). Toluene acts as a repellent for wild-type *E. coli* MG1655 already in the range of 60 to 200 μM (Fig. 4A). At lower benzoate concentrations, *E. coli* MG1655 chemotaxis is not significantly perturbed, and cells expressing the PcaY receptor showed a net positive attraction to 300 μM benzoate (1.5- to 2.0-fold compared to the accumulation of *E. coli* MG1655 on 300 μM benzoate).

We conclude, albeit carefully, that the *E. coli* chemoattractant repertoire can be expanded to aromatic compounds by heterologous expression of *P. putida* type 40H chemoreceptors. It could potentially be interesting to use *E. coli* chemotaxis for quantitative sensing of chemicals, because of the relatively rapid response time (5 to 30 min in microfluidic assays [3]) and its potentially narrower detection selectivity than that the original host bacteria. For instance, depending on the strain, *P. putida* encodes 20 to 30 potential chemoreceptors with partially overlapping chemoattractants (9, 10), compared to *E. coli*, with only five chemoattractants. Quantification of cell accumulation

TABLE 1 Strains used in this study

Strain lab collection no.	Host	Plasmid	Relevant characteristics	Source or reference
88	*P. putida* F1		Used as source for *pcaY*	36
1127	*P. putida* MT53	pWW53	Used as source for *mcpT*	23
3396	*E. coli* DH5α	pBAM-link-mcherry	Peptide-linker-*mcherry* coding sequence	32
4498	*E. coli* MG1655		Verified for motility	*E. coli* Genetic Center, Yale (CGSC#8237)
5396	*E. coli* Δ*tsr*		MG1655 derivative in which the *tsr* gene was deleted	This study
5186	*E. coli* DH5α	pGEM-t-Easy-*trgp*-mcp	Amplified and cloned *trg* promoter from MG1655 plus first 12 bp of *mcpT*	This study
5197	*E. coli* MG1655	pCRO20	*trgp-mcpT* in pSTV28	This study
5447	*E. coli* MG1655	pCRO33	*trgp-pcaY* in pSTV28	This study
5448	*E. coli* MG1655	pCRO34	*trgp-tsr* in pSTV28	This study
5457	*E. coli* MG1655	pSTV28	Cloning vector	TaKaRa, Japan
5775	*E. coli* MG1655	pCRO35	*trgp-mcpT*$_{FS}$ in pSTV28, frameshift mutation in *mcpT* coding sequence	This study
5782	*E. coli* MG1655	pCRO36	*trgp-mcpT-mcherry* fusion on pSTV28	This study
5839	*E. coli* MG1655	pCRO37	Same as pCRO36 but with a frameshift mutation in *mcpT*	This study
5841	*E. coli* MG1655	pCRO38	*trgp-tsr-mcherry* fusion on pSTV28	This study
5924	*E. coli* MG1655	pCRO33-mChe	*trgp-pcaY-mcherry* fusion on pSTV28	This study
6085	*E. coli* Δ*tsr*	pCRO20	Strain 5396 carrying *trgp-mcpT*	This study
6068	*E. coli* Δ*tsr*	pCRO33	Strain 5396 carrying *trgp-pcaY*	This study
5846	*E. coli* Δ*tsr*	pCRO36	Strain 5396 carrying *trgp-mcpT-mcherry*	This study
6010	*E. coli* Δ*tsr*	pCRO33-mChe	Strain 5396 carrying *trgp-pcaY-mcherry*	This study
6013	*E. coli* Δ*tsr*	pCRO38	Strain 5396 carrying *trgp-tsr-mcherry*	This study

as a function of chemoattractant concentration may further be improved by using microfluidic platforms in which stable chemical gradients can be produced, as we have recently shown (3). However, if heterologously expressed chemoreceptors in *E. coli* are to be used for quantitative sensing of chemoattractants, their compatibility with the existing *E. coli* chemotaxis machinery has to be improved. For that matter, an alternative and successful approach recently showed that functional hybrid receptors can be expressed in *E. coli* by fusing noncognate ligand-binding domains to the signaling domain of its chemoreceptors. Reactions to ligands can be measured by Förster resonance energy transfer between CheY and CheZ (30, 31). The existing *E. coli* chemotaxis machinery can thus be expanded both by hybrid and heterologous chemoreceptors and could pave the way for future faster and selective biosensors.

MATERIALS AND METHODS

Cloning procedures. The gene for the methyl-accepting chemotaxis receptor (*mcpT*) was amplified from *P. putida* MT53(pWW53) (23) (Table 1) genomic DNA by using Q5 proofreading polymerase (New England BioLabs) and primers 141001 and 141002 (Table 2). The forward primer 141001 contained a BamHI restriction site, and the reverse primer 141002 was elongated with a ClaI restriction site. The PCR fragment was cloned into pGEM-T Easy (Promega), and the insert was verified by sequencing (Fig. S3). The *trg* promoter of the *E. coli* chemoreceptor gene for Trg was amplified from *E. coli* MG1655 genomic DNA using a Q5 proofreading polymerase and primers 150613, elongated with a BamHI site, and 150612, with a SacI restriction site and including the 17-bp 5′ part of *mcpT* until its internal NheI site (Fig. S3). The *trg* promoter fragment was inserted upstream of the *mcpT* sequence in pGEM-T Easy by digestion with BamHI and NheI, taking advantage of an *mcpT*-internal NheI site (Fig. S2). The correct fragment was finally inserted into pSTV28 by digestion with SacI and ClaI, and the plasmid was renamed pCRO20 (Table 1 and Fig. S2 and S3). This plasmid was inserted into a verified motile strain of *E. coli* MG1655 (*E. coli* Genetic Center, Yale, CGSC#8237; Table 1).

A frameshift mutation was introduced in *mcpT* to disrupt its coding sequence, by digestion of pCRO20 with NsiI, removal of the 3′-overhangs by treatment for 20 min at 12°C with T4 DNA polymerase (New England BioLabs), and recircularization of the plasmid with T4 DNA ligase. After transformation, this plasmid was renamed pCRO35 (Table 1 and Fig. S2).

An *mcpT-mcherry* fusion was produced by amplification of a "*linker-mcherry*" fragment from plasmid pBAM-link-mcherry (32) using primers 170239 and 170240 elongated with a BglII restriction site and the C-terminal part of *mcpT* until the internal MfeI site, respectively (Table 2 and Fig. S2). The *link-mcherry* fragment was inserted in pCRO20 by digestion with BglII and MfeI. This plasmid was renamed pCRO36 (Table 1 and Fig. S2).

The receptor gene for PcaY from *P. putida* F1 was also cloned under the control of the *trg* promoter on pSTV28. Its coding sequence (*Pput2149*) was amplified from *P. putida* F1 genomic DNA using primers 160306 and 160307, whereas the *trg* promoter was amplified using primers 150613 and 160305 (Table 2).

TABLE 2 Primers used in this study

Primer no.	Sequence (5′–3′)[a]	Primer specificity	Amplification target
141001	T**GGATCC**TCTAGAAATAATTTTGTTTAACTTTAAGAAGGAGATATACAT*ATG*AGTGGTTGGCTAGCCCGTTTCTCAATAAAAACC	BamHI restriction site	*mcpT* from *P. putida* MT53
141002	ATTGGCAACGGTCAGCTTT**ATCGAT**GGAGATCTCACTAAAGACGGAACATGTGCATCAGACGCTGAA	ClaI restriction site	*mcpT* from *P. putida* MT53
150613	A**GGATCC**TCT**GAGCTC**CGGTTAGCCTGAAAACAG	BamHI and SacI restriction sites	P_{trg} from *E. coli* MG1655, position 1490209 in U00096
150612	*GGCTAGCCAACCACTCAT*TACCGTTGTCTCTCGTCCAGGTTTACTCC	N-terminal part of *mcpT* until NheI restriction site (in italics)	P_{trg} from *E. coli* MG1655, position 1490493 in U00096, specific for *mcpT* cloning
170239	TTTTT**AGATCT**TTATTTGTACAGCTCATCCATGCC	BglII restriction site	*Linker-mcherry* to fuse with *mcpT*
170240	CG**CAATTG**GCTTCTCTGGCAAGCCAACTTCAGCGTCTGATGCACATGTTCCGTCTTAAGCTTCCGGAAAATTCGAACG	C-terminal part of *mcpT* until MfeI restriction site	*Linker-mcherry* to fuse with *mcpT*
160305	*GAATTTTCAGGTTGGCAAGCAT*TACCGTTGTCTCTCGTCCAGGTTTACTCC	Overlapping sequence with N-terminal part of *pcaY* (in italics)	P_{trg} from *E. coli* MG1655, specific for *pcaY* cloning
160306	ATGCTTGCCAACCTGAAAATTCGCACC	N-terminal part of *pcaY*	*pcaY* from *P. putida* F1 (Ppu_2149)
160307	C**ATCGAT**TCATCAAACCTTGAACCGCCCCACCAACG	ClaI restriction site	*pcaY* from *P. putida* F1 (Ppu_2149)
160308	*CAATTTTGATACGTTTTAACAT*TACCGTTGTCTCTCGTCCAGGTTTACTCC	Overlapping sequence with N-terminal part of *tsr* (in italics)	P_{trg} from *E. coli* MG1655, specific for *tsr* cloning
160309	ATGTTAAAACGTATCAAAATTGTGACC	N-terminal part of *tsr*	*tsr* from *E. coli* MG1655
160310	CATCGATTCATTAAAATGTTTCCCAGTTCTCC		*tsr* from *E. coli* MG1655
101003	GGGGAAGCTTCCGGAAAATTCGAACGTTACGCGTCACCGGTCGGCCACCGTTTCCAAGGGCGAGGAGG		*Linker-mcherry* to fuse with *tsr*
101004	GGGG**ACTAGT**TTATTTGTACAGCTCATCCATGCC	SpeI restriction site	*Linker-mcherry* to fuse with *tsr*
070418	CAGGAAACAGCTATGACC		P_{trg}-*tsr* from pCRO34
170931	GACAGCTTATCATCGTTATTTGTACAGCTCATCCATGCCG		Amplify and sew *pcaY-mcherry*
170932	AGGTTTGATGAATCGAAGCTTCCGGAAAATTCGAACG		Amplify and sew *pcaY-mcherry*

[a]Restriction sites are in bold type.

Both PCR fragments were fused by sewing PCR and cloned back into pSTV28 by digestion with SacI and ClaI. This plasmid was renamed pCRO33 (Table 1 and Fig. S2). To fuse the *pcaY* with the *mcherry* reading frame, pCRO33 was digested with ClaI and EcoRI, and the backbone was recovered. The *trg*-promoter-*pcaY* fragment was reamplified and combined with the *link-mcherry* fragment by sewing PCR, using primers 170931 and 170932. This fragment was then reinserted into the pCRO33-ClaI-EcoRI backbone using In-Fusion HD cloning (TaKaRa).

The *tsr* coding sequence was amplified from *E. coli* MG1655 genomic DNA using primers 160309 and 160310, whereas the *trg* promoter fragment was amplified using primers 150613 and 160308 (Table 2). Both fragments were fused by sewing PCR and subcloned into pGEM-T Easy. The complete part was then recovered and introduced into pSTV28 by digestion with SacI and PstI (localized in pGEM-T Easy). This plasmid was renamed pCRO34 (Table 1).

A *tsr-mcherry* fusion was produced by amplification of the *link-mcherry* fragment from pBAM-link-mcherry using primers 101003 and 101004, and a P_{trg}-*tsr* fragment from pCRO34 using primers 070418 and 160308 (Table 2). Both fragments were fused by sewing PCR, subcloned into pGEM-T Easy, and cloned back into pCRO34 by digestion with SacI and SpeI. This plasmid was named pCRO38 (Table 1). Relevant plasmids were then further transformed into *E. coli* MG1655 Δ*tsr* (strain 5396) with a complete deletion of *tsr* by double recombination.

Preparation of *E. coli* cultures for chemoattraction assays. *E. coli* strains were grown overnight at 37°C with 180 rpm shaking in M9 minimal medium supplemented with 4 g · liter^{-1} glucose, 1 g · liter^{-1} Bacto Casamino Acids (BD Difco), Hutner's trace metals (33), 1 mM $MgSO_4$, and 30 μg · ml^{-1} chloramphenicol (here called M9-Glc-Cm30). The cultures were diluted 100-fold in the morning in fresh M9-Glc-Cm30 and incubated for 3 h at 37°C with 180 rpm shaking until they reached exponential phase (culture turbidity at 600 nm, between 0.5 and 0.6). For chemoattraction assays, 1 to 5 ml of culture was centrifuged at 2,400 × *g* for 5 min, and the upper 0.9 ml of liquid was carefully removed (note that motile cells do not really sediment) and replenished with 1 ml of motility buffer (motility buffer is 10 mM potassium phosphate, 0.1 mM EDTA, 10 mM lactate [pH 7.0]) (34). This procedure was repeated once more, and finally, the cells were resuspended in 500 μl of motility buffer, yielding a density of ~10^9 cells · ml^{-1}.

For ISCAs, 5 ml of washed exponentially growing culture in M9-Glc-Cm30 was diluted in 300 ml preheated (37°C) motility buffer to obtain a cell concentration of 2 × 10^6 to 4 × 10^6 cells · ml^{-1}, and this suspension was used within 30 min. Note that we kept the washing procedure the same between both chemotaxis assays, although we noticed that directly diluting exponentially growing cells in motility buffer (without any centrifugation) increases the proportion of cells responsive to 100 and 300 μM serine in the ISCA by almost a factor of ten. This did not measurably influence the cell accumulation to toluene and benzoate.

Preparation of the chemoattractant sources. As positive control for *E. coli* chemotaxis, 1.4 ml of 2% dissolved agarose LE (analytical grade; Promega) solution at 55°C was supplemented with 0.15 ml of 1 mM serine solution in water (final serine concentration, 100 μM). The negative control consisted of 1.8% agarose solution in tap water. Further test sources for *E. coli* consisted of aspartate, *N*-methyl-D-aspartate, D-ribose, and D-galactose, with final concentrations of 10 and 100 μM.

To prepare the source of toluene, 1.8% agarose was dissolved in tap water and kept at 55°C. Two-milliliter Teflon-lined screw-cap glass vials (Supelco Analytical) were filled with 1.6 ml of melted 55°C agarose solution, into which was dissolved 10 μl of pure toluene. The toluene density is 0.87 g · ml^{-1}, and its molecular mass is 92.14 g · mol^{-1}; therefore, adding 10 μl toluene to 1.6-ml volume is equivalent to 8.7 mg per 1.6 ml to equal 5.4 mg · ml^{-1}. This corresponds to 60 mM. This toluene stock was serially diluted in prewarmed agarose by adding and mixing 0.15 ml of the agarose with the pure toluene source into 1.4 ml of 55°C agarose solutions and from there to further agarose solutions. The 10^{-3} dilution is thus equivalent to 60 μM. Toluene stocks were prepared fresh for every experiment.

Sources of benzoate were prepared by 100-fold dilution of a 1 M sodium benzoate stock in 1.8% 55°C agarose, which corresponds to a concentration of 10 mM benzoate. From here, benzoate was serially diluted in 55°C agarose to obtain stocks of 1 and 0.1 mM. All vials were kept tightly closed in a water bath at 55°C until preparing the chambers. Agarose solutions were prepared fresh for every experiment.

For ISCAs, the chemoattractants were diluted in motility buffer without agarose.

Chemoattraction assays using agarose plugs on microscope slides. While washing the cell cultures, the microscope source chambers were prepared (Fig. S1). Chambers consisted of a standard microscopy glass slide (Menzel Gläser, Thermo Scientific), onto which two small coverslips (24 by 24 mm, 0.13 to 0.17-mm thick, MGF-Slides) were deposited on both sides and maintained in place with ~10 μl of tap water. A drop of 4 μl of 55°C agarose solution with the chemoattractant source (see above) was deposited in the middle and immediately covered by a cleaned large coverslip (24 by 50 mm; Menzel Gläser) that bridges over the side coverslips and thus creates a chamber with a height of 0.17 mm.

A freshly grown and washed bacterial suspension in motility buffer was inserted around the agarose plug by pipetting 150 μl of cell suspension between the glass slide and the large coverslip. *E. coli* standard assays with serine and other known chemoattractants were carried out in triplicate in independent chambers. Toluene and benzoate assays were repeated in 4-fold replicates (one prepared *E. coli* culture, four independent chambers) in conjunction with positive (serine) and negative (no attractant added) controls. Toluene assays were further repeated on at least four independent occasions.

Bacterial accumulation was imaged after 15 min of incubation at room temperature (20 ± 2°C) using a DFC 350 FX R2 Leica camera mounted on an inverted DMI 4000 Leica microscope using a N Plan ×10 objective. This timing was based on parallel video imaging of agarose source assays with a Dino-Lite digital microscope at ×50 magnification (AnMo Electronics Corporation, Taiwan) (see Video S1 in the supplemental material). For each replicate, one image was taken at each side of the agarose plug. Images

were analyzed with ImageJ software (version 1.49r; http://imagej.nih.gov/ij). Cells were identified using the "find edges" routine in ImageJ, and the accumulated intensity values were quantified per zones of 25 pixels width (corresponding to 2.5 μm) parallel to the plug border (3 zones in the plug and 27 zones outside the plug; Fig. S1). Chemotactic responses were then averaged from four replicates. Intensity values were summed and averaged across the three zones closest to the source edge, and intensity variations among chemoattractants were analyzed in one-way ANOVA statistics.

ISCA. As an alternative independent approach to the agarose plug assays, we measured chemotaxis in the ISCA (21). An ISCA device consists of a polydimethylsiloxane (PDMS) structure bonded to a glass slide, forming five replicate circular wells, each having a volume of ~110 μl that connects to the outside through an acentrically placed 0.8-mm-diameter inlet port. Wells were filled through the inlet port with a chemoattractant solution to the top, with care to leave a small (5 μl) droplet on the surface of the inlet. The filled ISCA device was then placed in a petri dish, which was very slowly filled with 55 ml of a suspension of *E. coli* at a density of 2×10^6 to 4×10^6 cells $\cdot$ ml^{-1} (in motility buffer, preheated at 37°C) until the ISCA was completely submerged. After 35 min of incubation at room temperature (22°C), the external cell suspension was removed by pipetting, and the ISCA surface was wiped with a clean tissue. The contents of each ISCA well were collected with a 1-ml syringe and a clean needle, transferred to a 200-μl well of a flat-bottom 96-well culture plate, and mixed with 1 μl of a 1:100 dilution of SYBR green I for cell staining. Stained cell suspensions were kept on ice until all samples were obtained and then aspirated into a Becton Dickinson flow cytometer, operated at 30 μl $\cdot$ min^{-1} and counted over 60 s. From the cell counts (number of cells per microliter) determined by flow cytometry for each ISCA well, we computed the mean and the standard deviation across the five replicate wells. The results presented in Fig. 4 were then obtained by normalizing to the mean cell count obtained with the ISCA for the same strain on the same day over five replicate wells containing only motility buffer (no-chemoattractant control), to quantify the enhancement in cell concentration due to chemotaxis ("normalized accumulation").

Epifluorescence microscopy of fusion proteins. In order to visualize the localization of McpT-, Tsr- and PcaY-mCherry expressed in *E. coli* MG1655, strains were precultured with the same protocol as for the agarose plug assays. However, cells were resuspended in 50 μl of motility buffer after the final washing step. A drop of 7 μl of this cell suspension was spotted on a 1% (wt/vol) agarose (in motility buffer)-coated microscopy slide (layer thickness, 1 mm) and then covered with a regular 0.17-mm-thick glass coverslip. Cells were imaged at an exposure time of 50 ms (phase-contrast) or 750 ms (mCherry) with a Nikon Eclipse Ti-E inverted microscope, equipped with an ORCA-flash4.0 camera (Hamamatsu) and a Plan Apo λ100 $\times$1.45 oil objective (Nikon). Images were recorded in ImageJ, saved as 8-bit grayscale for reproduction, opened and cropped to their final size in Adobe Photoshop (version CC2017), and finally saved as .TIF with 300 dots per inch (dpi) resolution for display. Cells were automatically segmented using SuperSegger and standard *E. coli* parameter settings (35), and both cellular fluorescence and the fluorescence intensities, scores, and positions of up to 9 foci in individual cells were extracted. Foci surpassing a focus score of 9 were listed using an in-house MatLab script (version 2016a), and their positions were normalized to a standardized *E. coli* cell for accumulated display. For expression quantification, cells with outlier mean fluorescence levels ($<$5th and $>$95th percentiles) were removed, after which the top 10% pixel intensities per cell were extracted (assuming this would correspond to the mCherry fusion protein positions in foci or fluorescent bands) and averaged per cell, and further normalized by the cell's mean fluorescence. This list of normalized average top 10% pixels per cell was then multiplied by the average of all mean individual cellular fluorescence values for that strain and incubation, in order to allow for interstrain expression comparisons. Lists were randomly subsampled in 10 individual replicates, the means of which were used for ANOVA comparison among strains, followed by Tukey's *post hoc* testing of statistical significance, using the program R.

SUPPLEMENTAL MATERIAL

Supplemental material for this article may be found at https://doi.org/10.1128/AEM.01362-18.

SUPPLEMENTAL FILE 1, PDF file, 2.0 MB.

SUPPLEMENTAL FILE 2, MOV file, 0.4 MB.

ACKNOWLEDGMENTS

We thank Vitali Maffenbeier for his help in cloning the PcaY-mCherry fusion construct. We thank the Stocker Lab at the ETH Zürich for advice and training in the ISCA.

This work was supported by the Swiss National Science Foundation NanoTera project 20NA21-143082, by financing from the Herbette Foundation (grant 2018-1-D-26), and by a grant from the Gordon and Betty Moore Foundation (grant 3801 to R.S.).

We declare no conflicts of interest.

REFERENCES

1. Matilla MA, Krell T. 2017. Chemoreceptor-based signal sensing. Curr Opin Biotechnol 45:8–14. https://doi.org/10.1016/j.copbio.2016.11.021.

2. Roggo C, van der Meer JR. 2017. Miniaturized and integrated whole cell living bacterial sensors in field applicable autonomous devices.

Curr Opin Biotechnol 45:24–33. https://doi.org/10.1016/j.copbio.2016.11.023.
3. Roggo C, Picioreanu C, Richard X, Mazza C, van Lintel H, van der Meer JR. 2018. Quantitative chemical biosensing by bacterial chemotaxis in microfluidic chips. Environ Microbiol 20:241–258. https://doi.org/10.1111/1462-2920.13982.
4. Sourjik V, Wingreen NS. 2012. Responding to chemical gradients: bacterial chemotaxis. Curr Opin Cell Biol 24:262–268. https://doi.org/10.1016/j.ceb.2011.11.008.
5. Sourjik V, Armitage JP. 2010. Spatial organization in bacterial chemotaxis. EMBO J 29:2724–2733. https://doi.org/10.1038/emboj.2010.178.
6. Alexander RP, Zhulin IB. 2007. Evolutionary genomics reveals conserved structural determinants of signaling and adaptation in microbial chemoreceptors. Proc Natl Acad Sci U S A 104:2885–2890. https://doi.org/10.1073/pnas.0609359104.
7. Lacal J, Garcia-Fontana C, Munoz-Martinez F, Ramos JL, Krell T. 2010. Sensing of environmental signals: classification of chemoreceptors according to the size of their ligand binding regions. Environ Microbiol 12:2873–2884. https://doi.org/10.1111/j.1462-2920.2010.02325.x.
8. Szurmant H, Ordal GW. 2004. Diversity in chemotaxis mechanisms among the bacteria and archaea. Microbiol Mol Biol Rev 68:301–319. https://doi.org/10.1128/MMBR.68.2.301-319.2004.
9. Hazelbauer GL, Falke JJ, Parkinson JS. 2008. Bacterial chemoreceptors: high-performance signaling in networked arrays. Trends Biochem Sci 33:9–19. https://doi.org/10.1016/j.tibs.2007.09.014.
10. Sampedro I, Parales RE, Krell T, Hill JE. 2015. *Pseudomonas* chemotaxis. FEMS Microbiol Rev 39:17–46. https://doi.org/10.1111/1574-6976.12081.
11. Baraquet C, Theraulaz L, Iobbi-Nivol C, Mejean V, Jourlin-Castelli C. 2009. Unexpected chemoreceptors mediate energy taxis towards electron acceptors in *Shewanella oneidensis*. Mol Microbiol 73:278–290. https://doi.org/10.1111/j.1365-2958.2009.06770.x.
12. Watts KJ, Taylor BL, Johnson MS. 2011. PAS/poly-HAMP signalling in Aer-2, a soluble haem-based sensor. Mol Microbiol 79:686–699. https://doi.org/10.1111/j.1365-2958.2010.07477.x.
13. Herrera Seitz MK, Soto D, Studdert CA. 2012. A chemoreceptor from *Pseudomonas putida* forms active signalling complexes in *Escherichia coli*. Microbiology 158:2283–2292. https://doi.org/10.1099/mic.0.059899-0.
14. Parales RE, Harwood CS. 2002. Bacterial chemotaxis to pollutants and plant-derived aromatic molecules. Curr Opin Microbiol 5:266–273. https://doi.org/10.1016/S1369-5274(02)00320-X.
15. Krell T, Lacal J, Reyes-Darias JA, Jimenez-Sanchez C, Sungthong R, Ortega-Calvo JJ. 2013. Bioavailability of pollutants and chemotaxis. Curr Opin Biotechnol 24:451–456. https://doi.org/10.1016/j.copbio.2012.08.011.
16. Pandey G, Jain RK. 2002. Bacterial chemotaxis toward environmental pollutants: role in bioremediation. Appl Environ Microbiol 68:5789–5795. https://doi.org/10.1128/AEM.68.12.5789-5795.2002.
17. Parales RE, Luu RA, Hughes JG, Ditty JL. 2015. Bacterial chemotaxis to xenobiotic chemicals and naturally-occurring analogs. Curr Opin Biotechnol 33:318–326. https://doi.org/10.1016/j.copbio.2015.03.017.
18. Molina L, Duque E, Gomez MJ, Krell T, Lacal J, Garcia-Puente A, Garcia V, Matilla MA, Ramos JL, Segura A. 2011. The pGRT1 plasmid of *Pseudomonas putida* DOT-T1E encodes functions relevant for survival under harsh conditions in the environment. Environ Microbiol 13:2315–2327. https://doi.org/10.1111/j.1462-2920.2011.02492.x.
19. Lacal J, Munoz-Martinez F, Reyes-Darias JA, Duque E, Matilla M, Segura A, Calvo JJ, Jimenez-Sanchez C, Krell T, Ramos JL. 2011. Bacterial chemotaxis towards aromatic hydrocarbons in *Pseudomonas*. Environ Microbiol 13:1733–1744. https://doi.org/10.1111/j.1462-2920.2011.02493.x.
20. Luu RA, Kootstra JD, Nesteryuk V, Brunton CN, Parales JV, Ditty JL, Parales RE. 2015. Integration of chemotaxis, transport and catabolism in *Pseudomonas putida* and identification of the aromatic acid chemoreceptor PcaY. Mol Microbiol 96:134–147. https://doi.org/10.1111/mmi.12929.
21. Lambert BS, Raina JB, Fernandez VI, Rinke C, Siboni N, Rubino F, Hugenholtz P, Tyson GW, Seymour JR, Stocker R. 2017. A microfluidics-based *in situ* chemotaxis assay to study the behaviour of aquatic microbial communities. Nat Microbiol 2:1344–1349. https://doi.org/10.1038/s41564-017-0010-9.
22. Yu HS, Alam M. 1997. An agarose-in-plug bridge method to study chemotaxis in the Archaeon *Halobacterium salinarum*. FEMS Microbiol Lett 156:265–269. https://doi.org/10.1111/j.1574-6968.1997.tb12738.x.
23. Keil H, Keil S, Pickup RW, Williams PA. 1985. Evolutionary conservation of genes coding for *meta* pathway enzymes within TOL plasmids pWW0 and pWW53. J Bacteriol 164:887–895.
24. Alper H, Fischer C, Nevoigt E, Stephanopoulos G. 2005. Tuning genetic control through promoter engineering. Proc Natl Acad Sci U S A 102:12678–12683. https://doi.org/10.1073/pnas.0504604102.
25. Hollands K, Lee DJ, Lloyd GS, Busby SJ. 2010. Activation of sigma 28-dependent transcription in *Escherichia coli* by the cyclic AMP receptor protein requires an unusual promoter organization. Mol Microbiol 75:1098–1111. https://doi.org/10.1111/j.1365-2958.2009.06913.x.
26. Ping L, Weiner B, Kleckner N. 2008. Tsr-GFP accumulates linearly with time at cell poles, and can be used to differentiate 'old' versus 'new' poles, in *Escherichia coli*. Mol Microbiol 69:1427–1438. https://doi.org/10.1111/j.1365-2958.2008.06372.x.
27. Shiomi D, Banno S, Homma M, Kawagishi I. 2005. Stabilization of polar localization of a chemoreceptor via its covalent modifications and its communication with a different chemoreceptor. J Bacteriol 187:7647–7654. https://doi.org/10.1128/JB.187.22.7647-7654.2005.
28. Piñas GE, DeSantis MD, Parkinson JS. 2018. Noncritical signaling role of a kinase-receptor interaction surface in the Escherichia coli chemosensory core complex. J Mol Biol 430:1051–1064. https://doi.org/10.1016/j.jmb.2018.02.004.
29. Kihara M, Macnab RM. 1981. Cytoplasmic pH mediates pH taxis and weak-acid repellent taxis of bacteria. J Bacteriol 145:1209–1221.
30. Bi S, Pollard AM, Yang Y, Jin F, Sourjik V. 2016. Engineering hybrid chemotaxis receptors in bacteria. ACS Synth Biol 5:989–1001. https://doi.org/10.1021/acssynbio.6b00053.
31. Derr P, Boder E, Goulian M. 2006. Changing the specificity of a bacterial chemoreceptor. J Mol Biol 355:923–932. https://doi.org/10.1016/j.jmb.2005.11.025.
32. Miyazaki R, Minoia M, Pradervand N, Sulser S, Reinhard F, van der Meer JR. 2012. Cellular variability of RpoS expression underlies subpopulation activation of an integrative and conjugative element. PLoS Genet 8:e1002818. https://doi.org/10.1371/journal.pgen.1002818.
33. Gerhardt P, Murray RGE. 1981. Manual of methods for general bacteriology. American Society for Microbiology, Washington, DC.
34. Berg HC, Brown DA. 1974. Chemotaxis in *Escherichia coli* analyzed by three-dimensional tracking. Antibiot Chemother (1971) 19:55–78. https://doi.org/10.1159/000395424.
35. Stylianidou S, Brennan C, Nissen SB, Kuwada NJ, Wiggins PA. 2016. SuperSegger: robust image segmentation, analysis and lineage tracking of bacterial cells. Mol Microbiol 102:690–700. https://doi.org/10.1111/mmi.13486.
36. Gibson DT, Zylstra GJ, Chauhan S. 1990. Biotransformations catalyzed by toluene dioxygenase from *Pseudomonas putida* F1, p 121–133. *In* Silver S, Chakrabarty AM, Iglewski B, Kaplan S (ed), *Pseudomonas*: biotransformations, pathogenesis and evolving biotechnology. American Society for Microbiology, Washington, DC.